in multiple species

– Supplementary Material –

Tina Binderup[1,2,#], Raphaël Duivenvoorden[1,3,#], Francois Fay[1,4,#], Mandy M.T. van Leent[1], Joost Malkus[1], Samantha Baxter[1], Seigo Ishino[1], Yiming Zhao[1], Brenda Sanchez-Gaytan[1], Jun Tang[1,5], Giuseppe Carlucci[5,6], Serge Lyashchenko[5,7], Claudia Calcagno[1], Nicolas Karakatsanis[1], Georgios Soultanidis[1], Max L. Senders[1,8], Philip M. Robson[1], Venkatesh Mani[1], Sarayu Ramachandran[1], Mark E. Lobatto[1,9], Barbara A. Hutten[10], Juan F. Granada[11], Thomas Reiner[5,7], Filip Swirski[12], Matthias Nahrendorf[12], Andreas Kjaer[2], Edward A. Fisher[13], Zahi A. Fayad[1,*], Carlos Pérez-Medina[1,14], Willem J.M. Mulder[1,8,15,*]

[1] Translational and Molecular Imaging Institute, Icahn School of Medicine at Mount Sinai, New York, NY, USA
[2] Department of Clinical Physiology, Nuclear Medicine and & PET, and Cluster for Molecular Imaging, Department of Biomedical Sciences, Rigshospitalet and University of Copenhagen, Copenhagen, Denmark
[3] Department of Nephrology, Radboud Institute for Molecular Life Sciences, Radboud University Medical Center, Nijmegen, The Netherlands
[4] Institut Galien Paris Sud, Faculté de Pharmacie, CNRS, Univ. Paris-Sud, Université Paris-Saclay, Châtenay-Malabry, France
[5] Department of Radiology, Memorial Sloan Kettering Cancer Center, New York, NY, USA
[6] Bernard and Irene Schwarz Center for Biomedical Imaging, New York University, New York, NY, USA
[7] Department of Radiology, Weill Cornell Medical College, New York, NY, USA
[8] Amsterdam University Medical Centers, Dept. of Medical Biochemistry, University of Amsterdam, Amsterdam, The Netherlands
[9] Department of Radiology, Spaarne Gasthuis, Haarlem, The Netherlands
[10] Department of Clinical Epidemiology, Biostatistics and Bioinformatics, Amsterdam University Medical Centers, Amsterdam, the Netherlands
[11] CRF Skirball Center for Innovation, The Cardiovascular Research Foundation, Orangeburg, NY, USA
[12] Center for Systems Biology and Department of Radiology, Massachusetts General Hospital, Harvard Medical School, Boston, MA, USA
[13] Department of Medicine (Cardiology) and Cell Biology, Marc and Ruti Bell Program in Vascular Biology, New York University School of Medicine, New York, NY, USA
[14] Centro Nacional de Investigaciones Cardiovasculares Carlos III, Madrid, Spain
[15] Laboratory of Chemical Biology, Department of Biomedical Engineering and Institute for Complex Molecular Systems, Eindhoven University of Technology, Eindhoven, The Netherlands
[#] Equal contribution
[*] Address correspondence to:
Willem J.M. Mulder, willem.mulder@mssm.edu
Zahi A. Fayad, zahi.fayad@mssm.edu
Translational and Molecular Imaging Institute, Icahn School of Medicine at Mount Sinai

One Gustave L. Levy Place, Box 1234
New York, NY 10029, USA

	Composition (g)					Size	
Batch #	APOA1	Simvastatin	DMPC	MHPC	Recovery* (%)	d.nm	*Đ*
1	0.704	1.235	6.683	0.690	57.8	21.8	0.255
2	0.692	1.214	6.569	0.678	70.8	30.8	0.294
3	0.704	1.235	6.683	0.690	65.8	21.1	0.261
4	1.500	2.631	14.239	1.469	75.5	24.5	0.224
5	1.250	2.192	11.866	1.225	61.8	22.3	0.239
6	0.441	0.773	4.186	0.432	60.8	20.4	0.241
7	0.900	1.578	8.543	0.882	71.3	28.0	0.215
8	0.700	1.228	6.645	0.686	71.8	22.0	0.156

Table S1. Composition and size of different S-HDL batches prepared for this study.
*Based on simvastatin

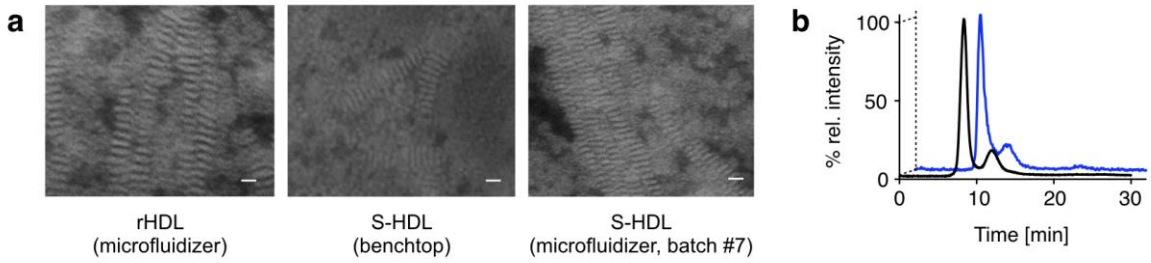

Fig. S1. a. Representative transmission electron microscopy (TEM) images of reconstituted high-density lipoprotein (rHDL, left), benchtop-produced simvastatin-HDL (S-HDL, middle) and microfluidizer-produced S-HDL (right). Scale bar = 10 nm. **b.** HPLC size exclusion chromatograms demonstrating co-elution of [^{89}Zr]-S-HDL (blue trace, radioactivity signal) and unlabeled S-HDL (black trace, UV absorption at 220 nm).

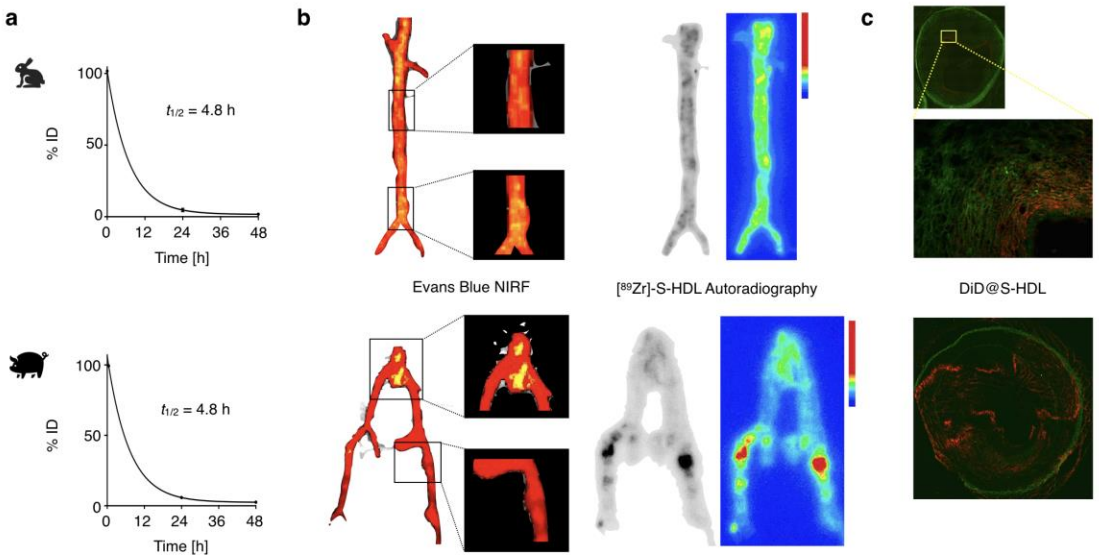

Fig. S2. a. Blood time–activity curve for [^{89}Zr]-S-HDL in rabbits (top, n=2) and pigs (bottom, n=2) with atherosclerosis. **b.** Representative Evans Blue near-infrared fluorescence imaging (left) and [^{89}Zr]-S-HDL autoradiography (right) performed on arterial samples from one rabbit (abdominal aorta, top) and one pig (femoral artery tree, bottom). **c.** Representative fluorescence microscopy images of arterial sections from one rabbit (top) and one pig (bottom) injected with DiD-S-HDL.

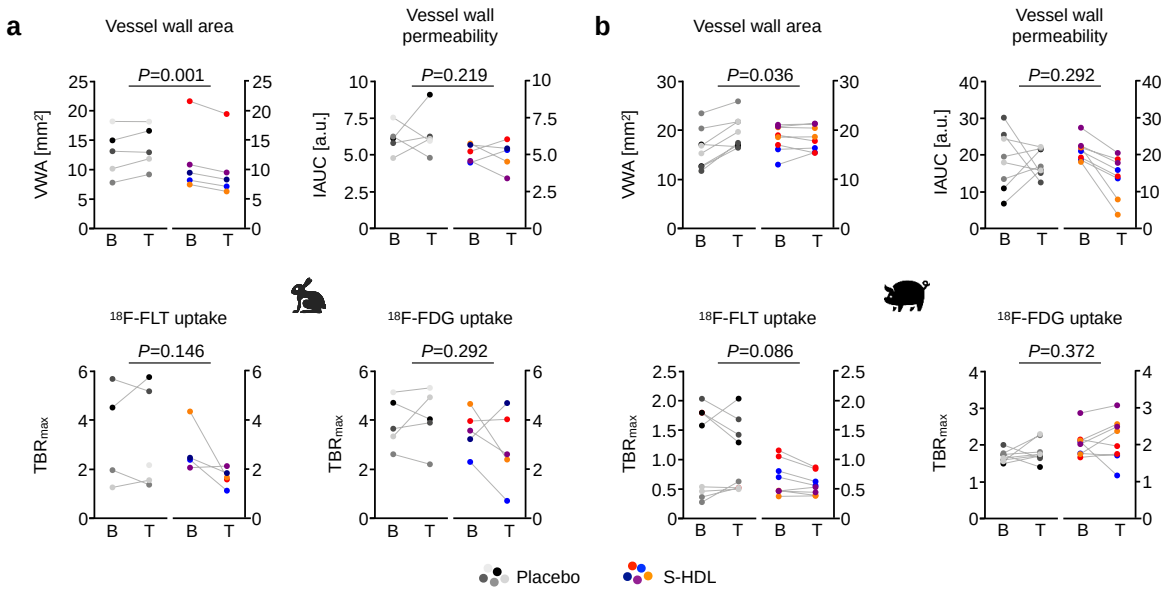

Fig. S3. a. Variation in the monitored parameters in rabbits treated with PBS (Placebo, red dots) or S-HDL (blue dots) between baseline (B) and terminal (T) scans. **b.** Variation in the monitored parameters in pigs treated with PBS (Placebo) or S-HDL between baseline (B) and terminal (T) scans. Dots are color-coded for individual animals. Two data points are represented per pig, corresponding to each of the femoral arteries. *P* values were calculated using the linear mixed model described in the manuscript. VWA = vessel wall area; IAUC = intensity area under the curve; TBR = target-to-background ratio.

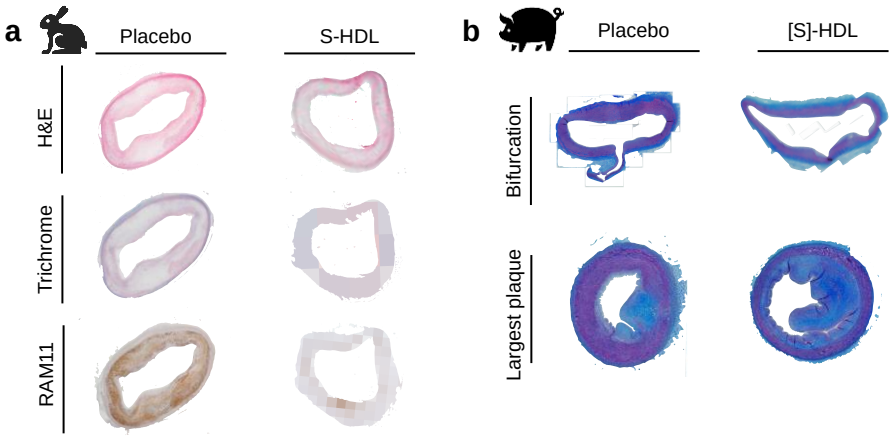

Fig. S4. a. Rabbit aortic sections stained with hematoxylin & eosin (H&E, top), Masson trichrome (middle) and RAM11 (macrophages, bottom) from animals treated with PBS (Placebo) or S-HDL. **b.** Porcine femoral artery sections (right) stained with Masson trichrome from animals

treated with PBS (Placebo) or S-HDL. Sections were taken from the iliac bifurcation (top) and largest plaque in the femoral artery (bottom) of the same pig.

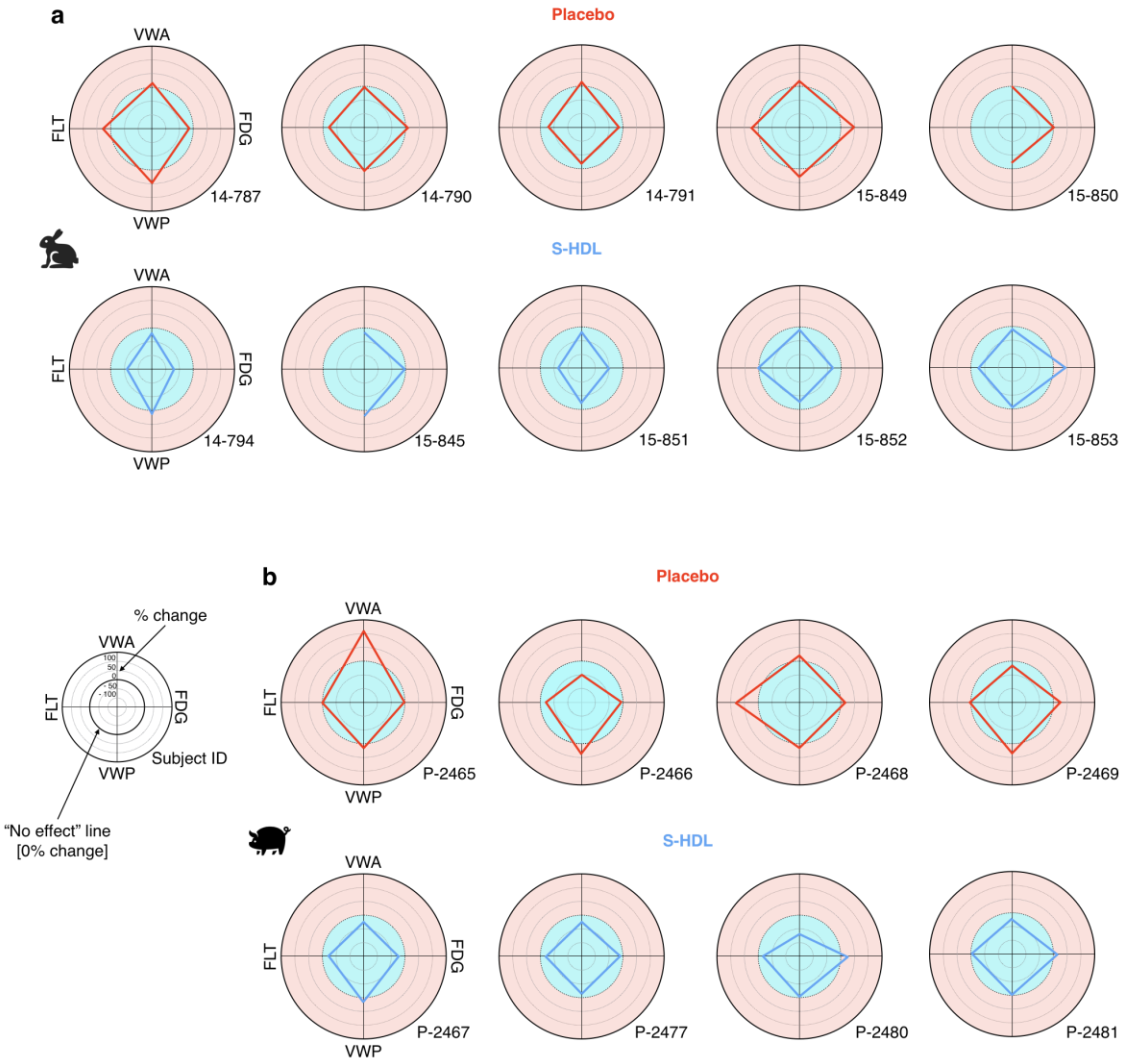

Fig. S5. a. Combined representation of the variation in the monitored parameters in individual rabbits treated with PBS (Placebo, top) or S-HDL (bottom), expressed as % change between baseline and terminal scans. **b.** Combined representation of the variation in the monitored parameters in individual pigs treated with PBS (Placebo, top) or S-HDL (bottom), expressed as % change between baseline and terminal scans. For FDG and FLT, data represent variation in TBR_{max}; VWA = vessel wall area; VWP = vessel wall permeability.